VII. References

[1] Alexander, R. McNeill, “Elastic Mechanisms in Animal Movement”, Cambridge University Press, 1988.

[2] Angle, C.M. and Brooks, R.A., “Small Planetary Rovers”, IEEE International Workshop on Intelligent Robots and Systems, Tsuchiura, Japan, July 1990 pp. 383-388.

[3] Asada, H. and Kanade, T. “Design of Direct-Drive Mechanical Arms”, ASME J. of Vibration, Acoustics, Stress, and Reliability in Design 105(3), pp. 312-316.

[4] Balas, Mark J., “Active Control of Flexible Systems”, Proc. of the 1977 Symposium on Dynamics and Control of Large Flexible Spacecraft, June 13-15, 1977, Blacksburg, VA pp 217-236.

[5] Brooks, R.A. and Stein, L.A., “Building Brains for Bodies”, to appear in Autonomous Robots, (1:1), 1994.

[6] Brooks, R.A., “The L Manual”, MIT AI Lab Internal, 1994.

[7] Cannon, Robert H. Jr., and Rosenthal, Dan E., “Experiments in the Control of Flexible Structures with Noncolocated Sensors and Actuators”, J. Guidance, Vol. 7 No. 5 pp. 546-553, Sept.-Oct. 1984.

[8] Cannon, Robert H. Jr., and Schmitz, E., “Initial Experiments on the End-Point Control of a Flexible One-Link Robot”, Int. J. of Robotics Research, Vol. 3 No. 3 (1984) pp 62-75.

[9] Eppinger, Steven D., and Seering, Warren P., “Three Dynamic Problems in Robot Force Control”, IEEE Intl. Conf. on Robotics and Automation, 1989, pp 392 - 397.

[10] Eppinger, Steven D., and Seering, Warren P., “Understanding Bandwidth Limitation in Robot Force Control”, IEEE Int. Conf. on Robotics and Automation, April 1987.

[11] Hashimoto, Minoru, and Imamura, Yuichi, “An Instrumented Compliant Wrist Using a Parallel Mechanism”, Japan/USA Symp. on Flexible Automation, V. 1 ASME 1992, pp 741-744.

[12] Hogan, N., “Impedance Control: An Approach to Manipulation: Part I - Theory, Part II - Implementation, Part III - Applications”, J. of Dyn. Syst., Measurement Contr., 107:1-24 (1985)

[13] Hogan, Neville, “On the Stability of Manipulators Performing Contact Tasks”, IEEE J. of Robotics and Automation, V4 N6, Dec. 1988, pp 677-686.

[14] Hogan, Neville, and Colgate, Ed, “An Analysis of Contact Instability in term of Passive Physical Equivalents”, IEEE Intl. Conf. on Robotics and Automation, 1989, pp 404-409.

[15] Hunter, Ian W., Hollerbach, John M., and Ballantyne, John, “A comparative analysis of actuator technologies for robotics”, Robotics Review 2, MIT Press, 1991.

[16] Khatib, O., “Real Time Obstacle Avoidance for Manipulators and Mobile Robots”, Int. J. of Robotics Res. V5 N1 (1986).

[17] Morrell, John B., and Salisbury, J. K., “Parallel Coupled Actuators for High Performance Force Control: A Micro-Macro Concept”, Submitted to IROS 95.

[18] Raibert, M. H., “Legged Robots That Balance.” Cambridge, Mass.: MIT Press (1986).

[19] Readman, Mark C., “Flexible Joint Robots”, CRC Press, 1994.

[20] Salisbury, K., Eberman, B., Levin, M., and Townsend, W., “The Design and Control of an Experimental Whole-Arm Manipulator”, Proc. 5th Int. Symp. on Robotics Research. (1989)

[21] Spong, M. W., “Modeling and Control of Elastic Joint Robots”, Trans. of the ASME, Vol 109, Dec. 1987, pp 310-319.

[22] Sugano, S., Tsuto, S., and Kato, I., “Force Control of the Robot Finger Joint equipped with Mechanical Compliance Adjuster”, Proc. of the 1992 IEEE/RSJ Int. Conf. on Intelligent Robots and Systems, 1992, pp 2005-2013.

[23] Whitney, Daniel E., “Force Feedback Control of Manipulator Fine Motions”, J. Dyn. Syst. Measurement Contr. 98:91-97 (1977)

[24] Whitney, Daniel E., “Historical Perspective and State of the Art in Robot Force Control”, Int. J. of Robotics Research, V6, N1, Spring 1987 pp 3-14.

imum possible force magnitude. Tests were performed at 12, 25, 38 (resonance) and 44 rad/sec.:

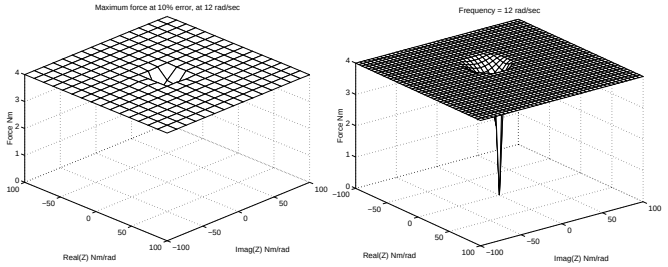

Fig. 10. Maximum output force vs. load impedance at 12 rad/sec

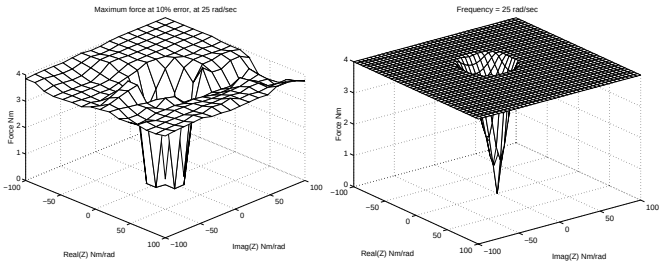

Fig. 11. Maximum output force vs. load impedance at 25 rad/sec

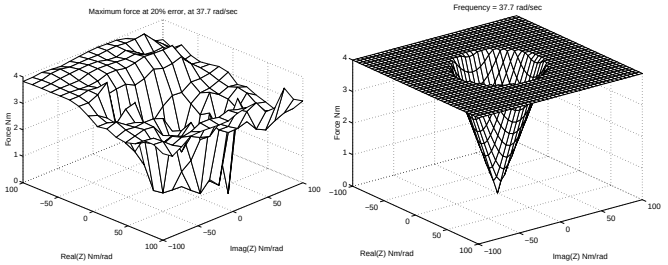

Fig. 12. Maximum output force vs. load impedance at 38 rad/sec

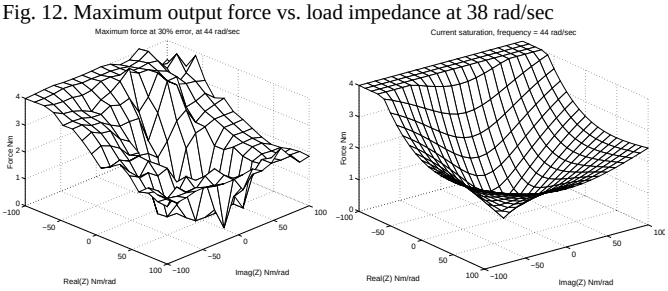

Fig. 13. Maximum output force vs. load impedance at 44 rad/sec

At low frequencies, performance is quite good The small downward spike corresponds to the lowest impedance that could be generated on the test rig without large-motion saturation. At resonance, performance at low impedances degrades, while at larger impedances performance is still good. Above resonance, it can clearly be seen that the actuator only performs well when its output impedance has a negative real part, which corresponds to positive spring-like behavior.

VI. Conclusions

Series-elastic actuators are presently being utilized in two research robots, and a third is now under construction. The first robot is Cog[5], whose arms are powered by revolute series-elastic actuators very similar to those used in the above tests. Another robot - a planer biped walker named “Spring Turkey” - utilizes series-elastic tendons to drive its leg joints. The limbs of both of these robots are shown below:

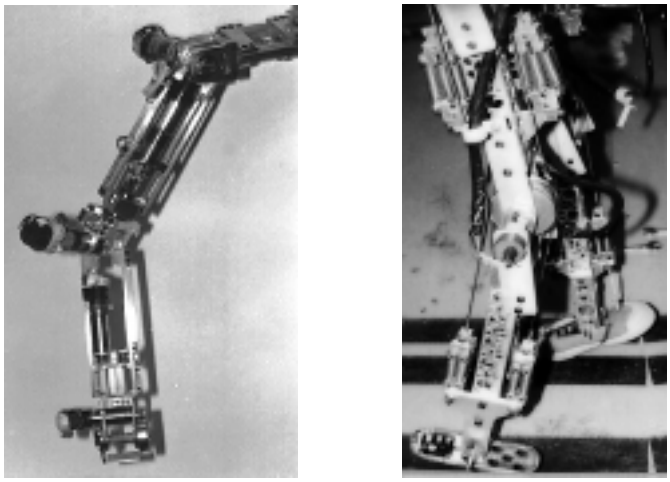

Fig. 14. One of Cog ‘s Arms (left) and Spring Turkey’s Legs (right)

A series-elastic arm for a small planetary rover is presently under construction.

In early system tests, both Cog’s arm and Spring Turkey’s legs have demonstrated performance that verifies the advantages of series-elastic actuators. Both robots interact with the environment under force or impedance control without any instability during transient contact with hard surfaces. Both robots have (so far) been robust to shock (presently more often a result of control programming errors than the environment). Spring Turkey has recently taken a few steps, showing that walking with series-elastic actuators is feasible

We believe that for natural tasks (such as walking and manipulation), series elastic actuators provide many benefits when compared to traditional actuators. These benefits include shock tolerance, lower reflected inertia, more accurate and stable force control, less damage during inadvertent contact, and energy storage. Although zero motion force bandwidth is reduced, force bandwidth for many tasks that involve load motion is improved. This is particularly true for natural tasks that are spring- or damper-like in their impedance[22].

We have shown that a simple control system can generate a range of complex output impedances - not just that of the passive series elasticity, and have demonstrated experimentally that accurate, stable control is easy to achieve.

Several avenues are open for future work, including parallel connections that extend both dynamic range and bandwidth [17] and variable-rate springs whose modulation of bias point can effect changes in passive stiffness. This type of mechanism has been studied before[21] and a more sophisticated version is currently being investigated at MIT by Ken Salisbury’s group and that of the authors.

$$Z = \frac{F_l}{X_l} = \frac{K_s(1-K_b)M_m\omega^2}{K_s(PID(j\omega)+1) - M_m s^2} \quad (6)$$

If the imaginary part of this impedance is less than or equal to zero, than the actuator as whole will be passive and thus stable when interacting with any passive load[13][14]. The only imaginary component of the impedance comes from the PID term, which is in the denominator. Thus, for the impedance to have a negative imaginary part, the PID term must have a positive imaginary part, i.e.:

$$\text{imag}\left(K_p + \frac{K_d j\omega}{1+\tau_d j\omega} + \frac{K_i}{1/\tau_i + jw}\right) \geq 0 \quad (7)$$

which is guaranteed for all ω when

$$\tau_i \leq \sqrt{\frac{K_d}{K_i}} \quad (8)$$

i.e., when the integral gain is rolled off below a sufficiently high frequency.

In a real system with motor saturation, the actuator will take on the natural impedance of the series elasticity at sufficiently high frequencies[10]. Thus, a light load mass may resonate with the series elasticity. To avoid this problem, placing a minimum mass on the load will lower the resonant frequency to where the control loop operates well. At this low frequency, the impedance of the series elasticity disappears from the overall impedance (which is very low), and resonance cannot occur.

IV. Experimental Setup

To evaluate performance, a series elastic actuator, shown in the photograph below, was constructed:

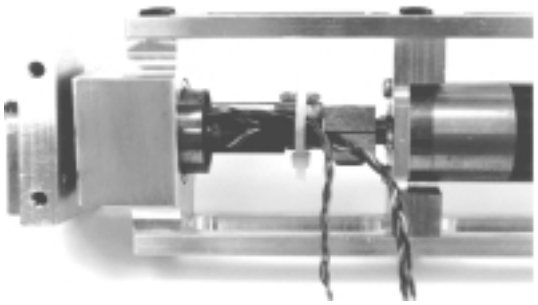

Fig. 8. Experimental Series-Elastic Actuator

The motor used was a MicroMo 3557K (48V, 25W) with a 66:1 reduction planetary gearbox. The gearbox's output shaft was attached to a steel torsion spring, which formed the series elasticity. The actuator output was taken from the other end of the spring. The spring was of a cross-shaped cross-section, which was found to give the best stiffness v. strength characteristics. The inertia of the motor at the output of the gearbox was calculated to be 0.02 kgm^2 and the stiffness of the spring was 34 Nm/rad, making the natural frequency of the system 41 rad/s or about 7Hz. The twist in the spring was measured using strain gauges mounted on the flats of the spring.

The control loop used was similar to that shown in fig. 6, only the $\frac{M_m s^2}{K_s}$ term was not implemented. The control parameters were set as follows:

K_p	12.41
K_i	12.41
τ_i	0.08
K_d	0.124
τ_d	.0015

A controlled load impedance was implemented by connecting the series elastic actuator's output to a conventional position-controlled motor, as shown below:

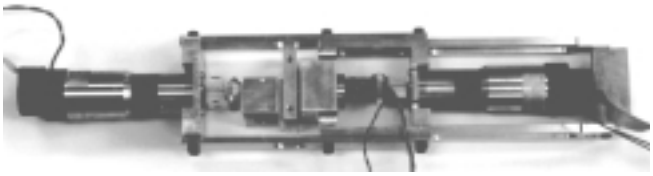

Fig. 9. Dual actuator test rig

V. Results

Both force and position were commanded sinusoidally at the same frequency, while magnitude and relative phase were varied. The performance was measured by calculating the root mean square force error and normalizing with respect to the commanded force amplitude. By then limiting RMS force error to a specific value, plots of the maximum possible output force magnitude over a range of output impedences were made. These were compared to the theoretical maximums given by equation 4, modified to take into account motor efficiency. In the plots below, the left plots show measured performance, the right show theoretical predictions. In each plot, the horizontal plane is impedance and the vertical axis is max-

Ignoring velocity saturation, we can compute performance by imposing a limit on the magnitude of F_m , i.e. $|F_m| < F_{max}$. For most motors, this translates into a bound on the maximum motor current. It is helpful to draw a vector diagram showing the magnitude and phase relationship of F_l and X_l, and the resulting F_m:

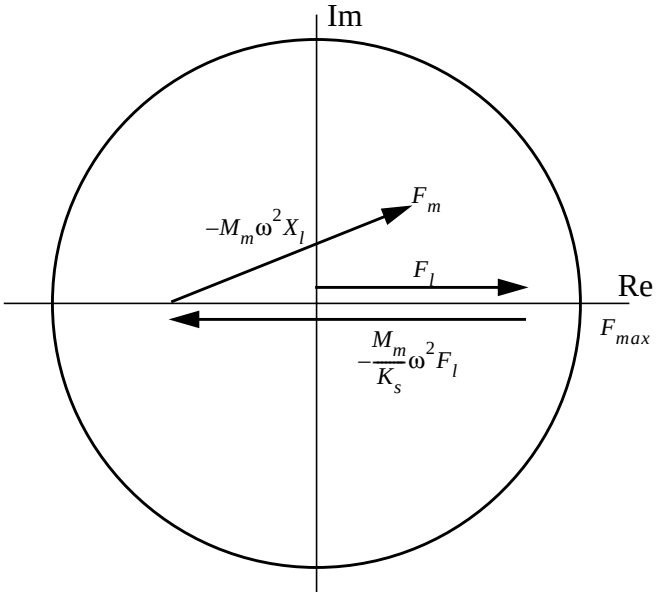

Fig. 5. Phase Diagram of Necessary Motor Force

Here we have arbitrarily aligned F_l with the real axis. To satisfy $|F_m| < F_{max}$, end point F_m must land inside the circle of radius F_{max}. Note that the series elasticity term $-\frac{M_m}{K_s}\omega^2 F_l$ opposes the F_l vector. Thus, for all frequencies below $\sqrt{2\frac{K_s}{M_m}}$, the series elasticity will bring the starting point of the $-M_m\omega^2 X_l$ vector closer to the circle's center and thus allow for a greater range of possible motion amplitudes and phases than would be possible with a stiff interface. If impedance control[12] is used, the $-M_m\omega^2 X_l$ term of the vector sum will point to the right when simulating positive rate springs, and thus the inclusion of series elasticity will improve actuator performance. At frequencies less than $\sqrt{2\frac{K_s}{M_m}}$, the maximum force amplitude of damping impedances, such as are used in damping control[22], is also increased.

It is also informative to consider actuator output force as a function of the output impedance $Z = \frac{F_l}{X_l}$ and motor force:

$$F_l = \frac{F_m Z}{\left(1 - \frac{M_m}{K_s}\omega^2\right) Z - M_m\omega^2} \tag{4}$$

This equation is plotted against actual test data later in the paper.

III. Control

Stable, accurate, force control can be obtained by using the architecture shown below, where F_d is the desired force:

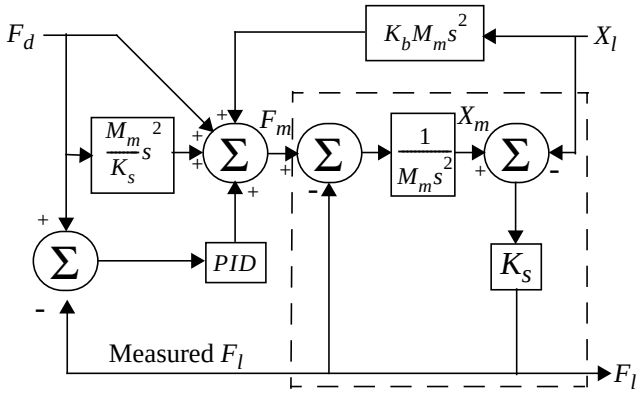

Fig. 6. Control Architecture

The feed-forward paths attempt to fully compensate for all three terms of equation 3, with the exception of the last (load motion) term, where a gain K_b is made less than 1 so as to prevent feedback inversion and instability.

Feedback to compensate for modeling errors and $K_b < 1$ is accomplished by an ordinary PID loop, operating on force error. This loop has a transfer function of:

$$PID(s) = K_p + \frac{K_d s}{1 + \tau_d s} + \frac{K_i}{1/\tau_i + s} \tag{5}$$

with parameters defined as follows:

K_p	Proportional Gain
K_i	Integral Gain
τ_i	Integral Roll-Off
K_d	Derivative Gain
τ_d	Derivative Roll-off

Fig. 7. Feedback Parameters

Stability can be analyzed by looking at the output impedance as a function of frequency $s = j\omega$ with a commanded force $F_d = 0$:

Series elasticity allows this trade-off to be driven much further towards high friction and low backlash, resulting in better position control at the gear train's output and thus better force control at the load. Importantly, high friction, low backlash gear trains can also be made inexpensively.

Increased series elasticity also makes stable force control more easy to achieve. Contrary to the case in position control, stable force control is easier to achieve when the frequency of interface resonances are **lowered**. This is because force feedback works well at low frequencies, creating a virtual zero-rate spring in series with the non-zero mechanical elasticity (i.e. a net spring rate of zero).

Finally, series elasticity provides for the possibility of energy storage. In legged locomotion, such energy storage can significantly increase efficiency[1]. By incorporating elasticity into the actuator package, efficiency benefits can be had despite the elasticity being hidden from the higher level control system. In other words, unlike methods that try to account for link elasticity at a systems level[19][20], the high level control system thinks it is controlling independent force actuators when in fact those actuators have internal springs that provide the aforementioned benefits.

Several authors have previously studied methods for controlling unavoidably flexible structures (such as those expected in space[4]), and the role of interface compliance in stabilizing force control during contact transitions[23]. But with the exception of systems where energy-storage is paramount (such as the legs of a hopping robot[18]), and some passive hand mechanisms[21][11], few have suggested that elasticity should be incorporated into general purpose robotic actuators. This seems strange, particularly for robots executing natural tasks, because elasticity is used for a wide variety of purposes in animals[1].

II. Performance Limits

Series elasticity creates the need for elastic deformation of the series element whenever force is modulated. This extra motion may add either constructively or destructively to the motion of the load. Thus, depending on the relative amplitude and phase of the load's force and motion waveforms, it is possible for the interface elasticity to either increase or decrease bandwidth.

Ignoring output inertia, a series-elastic actuator can be modeled as follows:

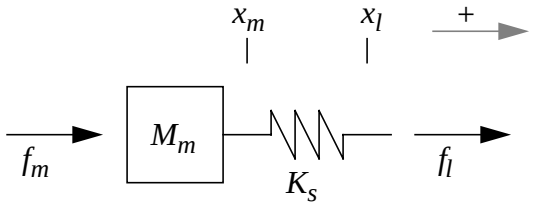

Fig. 2. Model of a series-elastic actuator

with the following frequency-domain system diagram:

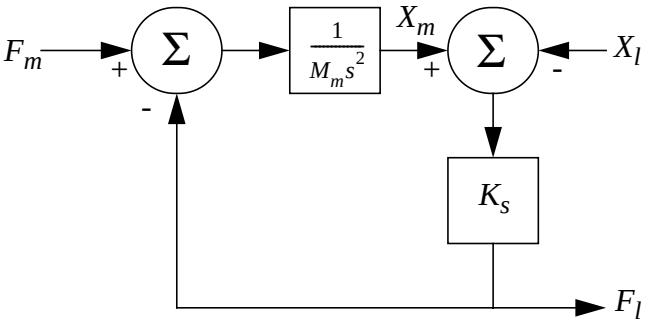

Fig. 3. Frequency Domain System Diagram

and the following variable definitions:

f_m , F_m	Magnetic Force Applied to Motor Rotor
f_l , F_l	Force Applied to Load
x_m , X_m	Position of Motor
x_l , X_l	Position of Load
M_m	Motor Mass
K_s	Elasticity Spring Rate

Fig. 4. System Variables

From the diagram above we can derive the following equations:

$$F_l = K_s (X_m - X_l) \tag{1}$$

$$X_m = \frac{F_m - F_l}{M_m s^2} \tag{2}$$

Setting $s = j\omega$ and solving for F_m , in terms of F_l and X_l we have:

$$F_m = F_l - \frac{M_m}{K_s}\omega^2 F_l - M_m \omega^2 X_l \tag{3}$$

As can be seen above, the motor force has three components. The first, F_l , is the force applied through the elasticity to the load. The second, $-\frac{M_m}{K_s}\omega^2 F_l$, is the force required to accelerate the motor's mass in order to change the deformation of the elasticity. The third, $-M_m \omega^2 X_l$, is the force required to accelerate the motor's mass so as to track motion of the load. Of these three terms, only the middle one is unique to the series elastic actuator.

Preprints of the Fourth International
Symposium on Experimental Robotics, ISER '95
Stanford, California, June 30-July 2, 1995

Stiffness Isn't Everything

Gill A. Pratt, Matthew M. Williamson, Peter Dillworth, Jerry Pratt, Karsten Ulland, Anne Wright
MIT Artificial Intelligence Laboratory and Laboratory for Computer Science

Abstract

Most robot designers make the mechanical interface between an actuator and its load as stiff as possible[9][10]. This makes sense in traditional position-controlled systems, because high interface stiffness maximizes bandwidth and, for non-collocated control, reduces instability. However, lower interface stiffness has advantages as well, including greater shock tolerance, lower reflected inertia, more accurate and stable force control, less damage during inadvertent contact, and the potential for energy storage. The ability of series elasticity (usually in the form of a compliant coating on an end-effector) to stabilize force control during intermittent contact with hard surfaces is well known. This paper proposes that for natural tasks where small-motion bandwidth is not of paramount concern, actuator to load interfaces should be significantly less stiff than in most present designs. Furthermore, by purposefully placing the majority of interface elasticity inside of an actuator package, a new type of actuator is created with performance characteristics more suited to the natural world. Despite common intuition, such a series-elastic actuator is not difficult to control.

After an analytic treatment of the trade-offs and limitations of series elastic actuators, we present a simple hybrid feed-forward / feed-back control system for their use. We conclude with test results from a revolute series-elastic actuator being used in the arms of the MIT humanoid robot Cog[5] and also in the arm of a small planetary rover[1]. A similar concept, but with pulley driven series-elastic tendons, is presently being used in a 2-D walking biped named "Spring Turkey".

I. Introduction

Robot designers have traditionally maximized the interface stiffness between actuators and loads[19], and with good reason. Stiffness improves the precision, stability, and bandwidth of position-control. When either open-loop positioning or collocated feedback are used, increased interface stiffness decreases end-point position errors under load disturbances. In non-collocated feedback systems (where the position sensor is located at the load side of the interface), increased stiffness both lowers necessary actuator motion in response to load variations and raises the resonant frequency of the motor inertia and interface compliance. As a result, stiffer interfaces allow the bandwidth of a position control feedback loop to be raised without compromising stability[7][8].

1. This work was supported by JPL contract # 959333, for which we are most grateful.

But stiffness isn't everything. Most electric motors have poor torque density and thus can deliver high power only at high speed[15]. To provide high power to slowly moving loads, gear reduction become necessary. Unfortunately, gears introduce friction and/or backlash, torque ripple, and noise. The use of N:1 gearing also causes an N^2 increase in reflected inertia so that shock loads cause very high stress on the teeth of the output gear, possibly resulting in failure. This increased reflected intertia and the typically high backdrive friction of high ratio gear trains can also cause damage to the robot or environment when unexpected contact occurs.

Reducing interface stiffness by inserting series elasticity can resolve many of these problems. The basic configuration of a series elastic actuator is shown below:

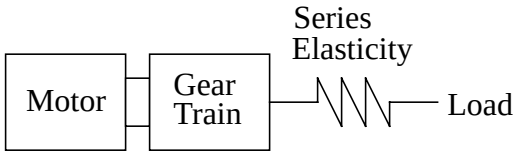

Fig. 1. Block Diagram of Series-Elastic Actuator

The first benefit of the series elasticity is to low-pass filter shock loads, thereby greatly reducing peak output gear forces. Although this also low-pass filters the actuator's output, we believe this is a place for an engineering trade-off, not the traditional "stiffer is better" minimization. The proper amount of interface elasticity can substantially increases shock tolerance while maintaining adequate small motion bandwidth for natural tasks like locomotion and manipulation.

Series elasticity also turns the force control problem into a position control problem, greatly improving force accuracy. In a series elastic actuator, output force is proportional to the position difference across the series elasticity multiplied by its spring constant. Because position is much more easy to control accurately through a gear train than force, the force errors usually caused by friction and torque ripple are reduced. Friction and backlash are usually a trade-off in gear train design.